

Synchronization of Voltage Stability in AVR-PSS using Fuzzy Logic Controller

Bibhu Prasad Ganthia¹, Amruta Abhisekh², Sarthak Biswal³, Satish Ranjan Sahu⁴, Dr. Subrat Kumar Barik⁵

¹ PhD Research Scholar, School of Electrical Engineering, KIIT University, India, jb.bibhu@gmail.com

² M.Tech, PSE, Electrical Engineering, IGIT, Sarang, Dhenkanal, Odisha, India, amrutaabhishek45@gmail.com

³ M.Tech, PSE, Electrical Engineering, IGIT, Sarang, Dhenkanal, Odisha, India, biswalsarthak02@gmail.com

⁴ M.Tech, PED, Electrical Engineering, IGIT, Sarang, Dhenkanal, Odisha, India, satishranjan543@gmail.com

⁵ Associate Professor, School of Electrical Engineering, KIIT University, India, skbarikfel@kiit.ac.in

ABSTRACT

The operation and stability of modern power systems have been threatened by the tremendous increase in the electrical energy usage. To meet the rising power demand, a large number of generators operate synchronously. Often electromechanical oscillations called power swings are induced by faults occurring within the system. A suitable damping device is needed to combat the loss of synchronism and other stability problems caused by these power swings. High performance excitation systems (AVR) with damper are well suited to maintain the steady state and transient stability of the generators in power system. In case of relatively weaker tie line interconnections between the power systems, low frequency oscillations are observed. These oscillations ranging from 0.5 – 3 Hz are quite common in the system. An effective means of improving the system damping of the electric power system is by using power system stabilizers. Effort has been given to develop a robust co-ordinate AVR-PSS using a fuzzy logic controller for an effective improvement in power system stability of a single machine system. In this work, a fuzzy logic based power system stabilizer has been designed for a single machine infinite bus power system. Simulation results indicate that the proposed fuzzy logic based coordinate AVR-PSS achieves a robust performance for a wide range of system operation conditions and offers superior performance over AVR-PSS without fuzzy logic controller.

Key words : SMIB, AVR, PSS, FLC, Exciter.

1. INTRODUCTION

Oscillations of small magnitude and low frequency often persist for long periods of time and sometimes can cause limitations in the power transfer capability. Power System Stabilizers (PSS) were developed to aid in damping these oscillations by modulating the excitation of generator. The art and science of applying power system stabilizers has been developed in the past thirty to thirty-five years since its first

widespread application to Western systems of the United States. The development has evolved the use of various tuning techniques and input signals and learning to deal with turbine generator shaft torsional mode of vibrations. Power System Stabilizers are added to the excitation system to enhance the damping of electric power system during low frequency oscillations. Several methods are used in the design of Power System Stabilizers. The classical methods include phase compensation and root locus method. The modern techniques make use of the state space representation of the power system model and calculate a gain matrix which when applied as a state feedback control will minimize a prescribed objective function. In recent years the limelight has been on designing PSSs using fuzzy logic based control techniques. Due to the geographically distributed nature of power system and lack of communication system (unavoidable delays) the decentralized control scheme may be more feasible than the centralized control scheme. In decentralized power system stabilizer, the control input for each machine should be function of the output of that machine only. This can be achieved by designing a decentralized PSS using periodic output feedback technique in which the gain matrix should have all the off-diagonal terms zero or very small compare to diagonal term. In this technique decentralized PSS for all machines can be described in one algorithm. All PSS can be applied simultaneously to the respective machine.

2. POWER SYSTEM MODELLING

The mathematical models for small signal analysis of synchronous machine excitation system and the lead-lag power system stabilizer are briefly reviewed. The general system configuration of synchronous machine connected to an infinite bus through transmission network can be represented as the Thevenin's equivalent circuit.

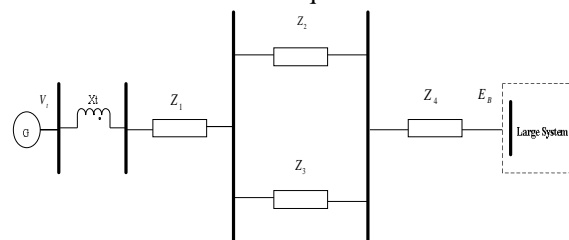


Figure.1: General Configuration of SMIB [1]

Initially the synchronous machine is represented by the classical model. Then the effects of the dynamics of the field circuit and the excitation system are taken into consideration. For analysis the figure 1 is reduced to the following figure 2.

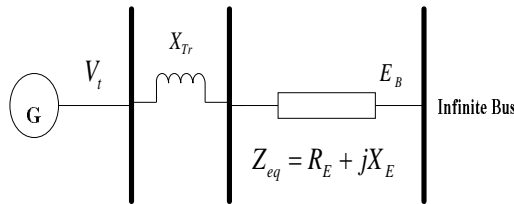


Figure.2: Equivalent Circuit of SMIB [1]

2.1 Single Machine Infinite Bus (SMIB) Model

$$S = P + jQ = E \cdot I^* = \frac{E' E_B \sin \delta}{X_t} + j \frac{E' (E' - E_B \cos \delta)}{X_t} \quad (1)$$

The equations of motion in per unit are

$$\begin{aligned} P \Delta \omega_r &= \frac{1}{2H} [\Delta T_m - K_S \Delta \delta - K_D \Delta \omega_r] \\ P \Delta \delta &= \omega_0 \Delta \omega_r \end{aligned} \quad (2)$$

Representing the eqn. (2.2) in matrix form we have,

$$\frac{d}{dt} \begin{bmatrix} \Delta \omega_r \\ \Delta \delta \end{bmatrix} = \begin{bmatrix} \frac{-K_D}{2H} & \frac{-K_S}{2H} \\ \omega_0 & 0 \end{bmatrix} \begin{bmatrix} \Delta \omega_r \\ \Delta \delta \end{bmatrix} + \begin{bmatrix} \frac{1}{2H} \\ 0 \end{bmatrix} \Delta T_m \quad (3)$$

Where, $\Delta \omega_r$ is the per unit angular speed deviation of the rotor.

- H is the inertia constant.
- T_m is the applied mechanical torque.
- K_D is the damping torque coefficient.
- δ is the rotor angle in electrical radians.
- ω_0 is the rotor speed in rad/sec.
- K_S is the synchronizing torque coefficient.

The synchronizing torque K_S is given by

$$K_S = \frac{E E_B \cos \delta_0}{X_t} \quad (4)$$

This is the state space representation of the form

$$\dot{X} = Ax + Bu$$

The elements of the state matrix are dependent on the system parameters H, K_D , X_T and the initial operating conditions represented by the values of \tilde{E}' and δ_0 . Vector B is also dependent on H.

Thus, the undamped natural frequency is given by

$$\begin{aligned} \omega_n &= \sqrt{K_S \frac{\omega_0}{2H}} \\ \zeta &= \frac{1}{2} \frac{K_D}{2H \omega_n} = \frac{1}{2} \frac{K_D}{\sqrt{K_S 2H \omega_n}} \end{aligned}$$

The natural frequency increases and the damping ratio increases with the decrease in the synchronizing torque.

An increase in the damping torque coefficient K_D increases the damping ratio, while an increase in the inertia constant decreases both ω_n and ζ .

2.2 Classical Model Representation of the Generator

The classical model representation of the generator neglecting all the resistances is given in fig. 3.

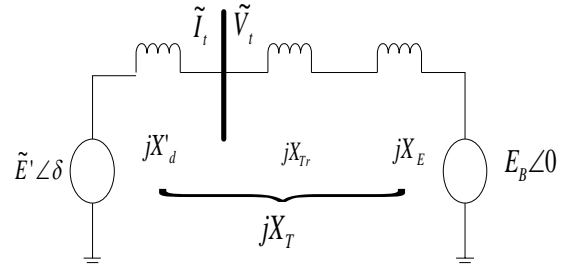


Figure.3. Classical model of the synchronous generator [2]

The magnitude of \tilde{E}' is assumed to be constant at the pre-disturbance value. Let δ be the angle by which \tilde{E}' leads the infinite bus voltage \tilde{E}_B .

2.3 Effects of the Excitation System

Now the effect of field flux variation is considered. Then the state space model of the system is developed, by first reducing the synchronous machine equations to an appropriate form and then combining them with the network equations.

In the classical generator model, the linearized equations of motions are

$$\begin{aligned} \frac{d}{dt} \Delta \omega_r &= \frac{1}{2H} (\Delta T_m - \Delta T_E - K_D \Delta \omega_r) \\ \frac{d}{dt} \Delta \delta &= \omega_0 \Delta \omega_r \end{aligned} \quad (5)$$

where ΔT_E is the electrical (air-gap) torque. The rotor angle δ is the angle (in electrical radians) by which the q-axis leads the reference E_B . The phasor diagram in fig. 3 shows the relative position of synchronous machine variables.

The rotor angle is given by

$$\delta = \delta_r + \delta_t \quad (6)$$

In fig. 3 δ_r is the angle by which the terminal voltage phasor V_t leads the reference E_B and the steady state value of δ is given by

$$\delta_r = a \cdot \tan \left(\frac{X_q \cos \phi - R_a I_t \sin \phi}{V_t + R_a I_t \cos \phi + X_d I_t \sin \phi} \right) \quad (7)$$

Where, V_t and I_t are terminal voltage and current.

ϕ is the power factor angle.

R_a is the armature resistance per phase.

X_q is the quadrature axis synchronous reactance.

The effect of field flux variations can be represented as

$$\frac{d}{dt} \Delta \varphi_{fd} = \frac{\omega_n R_{fd}}{L_{adu}} \Delta E_{fd} - \omega_n R_{fd} \Delta i_{fd} \quad (8)$$

where $\Delta \varphi_{fd}$ is the rotor circuit (field) flux linkage.

L_{adu} is the unsaturated direct-axis mutual inductance between stator and rotor windings.

E_{fd} is the exciter output voltage.

i_{fd} is the field circuit current.

In order to develop the complete system of equations in the state space form, ΔT_e and Δi_{fd} should be expressed in terms of the state variables as determined by the machine flux linkage equations and network equations. So, it can be written that

$$\begin{aligned} \Delta i_{fd} &= \frac{1}{L_{fd}} \left(1 + m_2 L_{ads} - \frac{L_{adv}}{L_{fd}} \right) \Delta \varphi_{fd} + \frac{1}{L_{fd}} m_1 L_{ads} \Delta \delta \\ (9) \quad L_{ads} &= \frac{L_{adv} L_{fd}}{L_{adv} + L_{fd}} \\ m_1 &= \frac{E_B (X_{Tq} \sin \delta_n - R_B \cos \delta_n)}{D} \\ m_2 &= \frac{X_{Tq}}{D} \left(\frac{L_{adv}}{L_{adv} + L_{fd}} \right) \\ R_T &= R_a + R_E \\ X_{Tq} &= X_{Tr} + X_E + (L_{ads} + L_l) \\ X_{Td} &= X_{Tr} + (L_{ads} + L_l) \\ D &= R_T^2 + X_{Tq} X_{Td} \quad (2.13) \end{aligned} \quad (10)$$

Where, X_{Tr} is the reactance of the transformer.

R_E is the Thevenin resistance of the network.

X_E is the Thevenin reactance of the network.

R_a is the armature resistance.

L_l is the leakage inductance of the stator.

L_{ads} is the saturated d-axis mutual inductance between stator and rotor windings.

L_{aqs} is the saturated q-axis mutual inductance between stator and rotor windings. Hence, it can be derived as

$$\Delta T_e = K_1 \Delta \delta + K_2 \Delta \varphi_{fd} \quad (11)$$

$\Delta \delta$ and ΔE depend on the prime mover and excitation controls. In case of constant mechanical input torque and $\Delta E = 0$.

3. POWER SYSTEM STABILITY

Power system stability can be broadly categorized into the following three types:

- Steady State Stability

This Analysis Deals With The Study Of The Power System And Its Components In Strictly Steady State Conditions, While Being Loaded To The Maximum Possible Extent Without Losing Synchronism With Each Other.

- Transient Stability

Transient Stability Is The Ability Of The Power System To Maintain Synchronism When Subjected To Sudden And Large Disturbances Within A Small Time Period (Usually 1 Second) Like Fault On Transmission Facilities, Loss Of Generation Etc. The System Response To Such Disturbances

Involves Large Excursions Of Generator Rotor Angles, Power Flows, Bus Voltages Etc.

- Dynamic Stability

Dynamic stability is said to be achieved by a system if the oscillations do not acquire a value which is higher than certain amplitude and die out quickly. This is used in the study of transient conditions in power systems. To describe the transient phenomena the swing equation derived from the torque equation of the synchronous machine can be used.

$$T_{mi} = \frac{d^2 \delta_i}{dt^2} = P_{Mi} - D_i \frac{d\delta_i}{dt} - P_{Ei} \quad (12)$$

Where, T_{mi} is the impulse moment of the rotor of the generating unit.

D_i is the damping coefficient (considering both the electrical and mechanical damping effect)

δ_i is the phase angle or load angle.

P_{Mi} is the turbine power applied to the rotor, and

P_{Ei} is the electrical power output from the stator.

4. AUTOMATIC VOLTAGE REGULATOR

The basic role of the AVR is to maintain the constancy in the generator terminal voltage under small and slow changes in the load. An exciter is the main component of the AVR loop. It delivers dc power to the generator field. The exciter is so designed with enough margins that it can provide powerful boosts in the excitation level even during emergency.

4.1 Exciter Type

A variety of exciter types have been in use since the old days. In the past, the power plants used to have exciters that consisted of a dc generator driven by the main generator shaft. This arrangement required the transfer of dc power to the generator via slip rings and brushes shown in figure 4.

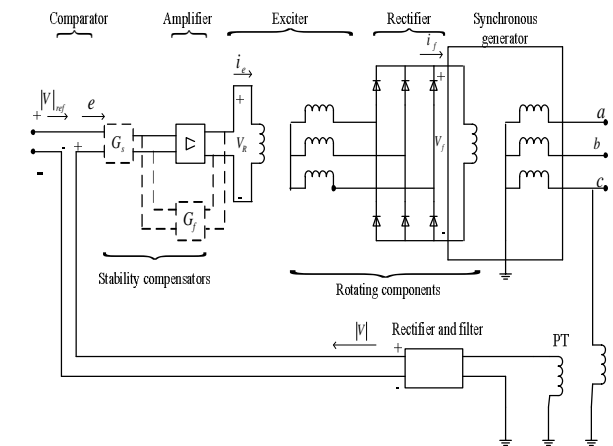


Figure.4:Brushless AVR Loop [4]

In the modern times, brushless or statically designed exciters are being used. In a brushless AVR a three phase inverted synchronous generator is used which has a three phase armature on its rotor and field on its stator. The diodes mounted on the rotating shaft rectify its ac armature voltage thus eliminating the need for slip rings and brushes. In a static AVR the excitation power is directly obtained from the

generator terminals or from the station service bus. The ac power is rectified by the thyristors bridges and fed to the main generator field via slip rings. These are extremely fast and contribute to the improved ‘transient stability’.

4.2 Exciter Modelling

The AVR loop from Figure 4 is described briefly here. Let the terminal voltage $|V|$ decreases for some reason which leads to immediate increase in the error voltage thereby causing increased v_R, i_e, v_f and i_f . As a result of the boost in the d-axis, the generator flux increases thus raising the magnitude of the internal generator emf E and terminal voltage V.

At the moment let the stability component for the comparator and amplifier be disregarded.

$$\Delta|V_{ref}| - \Delta|V| = \Delta e \tag{13}$$

$$\Delta v_R = K_A \Delta e \tag{14}$$

Where, K_A is the amplifier gain.

Laplace transformation of these two equations yield

$$|\Delta V_{ref}|(s) - \Delta|V|(s) = \Delta e(s) \tag{15}$$

$$G_A \cong \frac{\Delta v_R(s)}{\Delta e(s)} = K_A \tag{16}$$

Where, G_A is the amplifier transfer function.

Incorporating a delay represented by a time constant T_A in the above equation we have

$$G_A = \frac{\Delta v_R(s)}{\Delta e(s)} = \frac{K_A}{1+sT_A} \tag{17}$$

If R_e and L_e represent the resistance and inductance of the exciter field, we have for the voltage equilibrium

$$\Delta v_R = R_e + \Delta i_e + L_e \frac{d}{dt} (\Delta i_e) \tag{18}$$

The exciter produces K_e (armature) Volts per Ampere of field current i_e ; the proportionality is given by

$$\Delta v_f = K_e \Delta i_e \tag{19}$$

On eliminating Δi_e and performing Laplace Transformation of the last two equations the transfer function of the exciter is given by

$$G_e \cong \frac{\Delta v_f(s)}{\Delta v_R(s)} = \frac{K_e}{1+sT_e} \tag{20}$$

$$K_e \cong \frac{K_1}{R_e} \tag{21}$$

$$T_e \cong \frac{L_e}{R_e} \tag{22}$$

From the above equations and accepted block symbols the transfer function model of fig. 4.2 has been assembled. The time constants T_A and T_e range from 0.02-0.10 and 0.5-1.0 seconds.

4.3 Generator Modelling

The loop in figure 5 and figure 6 needs to be closed by establishing the missing dynamic link between the field voltage v_f and the generator terminal voltage $|V|$. The

relationship between v_f and $|V|$ depends on the generator loading as the terminal voltage is the result of the differences between internal emf and the voltage drop across internal impedance. At zero or low loading there exists the simplest possible relationship so that V is approximately equal to E. Applying Kirchoff’s voltage law to the field winding results in

$$\Delta v_f = R_f + \Delta i_f + L_{ff} \frac{d}{dt} (\Delta i_f) = \frac{\sqrt{2}}{\omega L_{fd}} [R_f \Delta E + L_{ff} \frac{d}{dt} (\Delta E)] \tag{23}$$

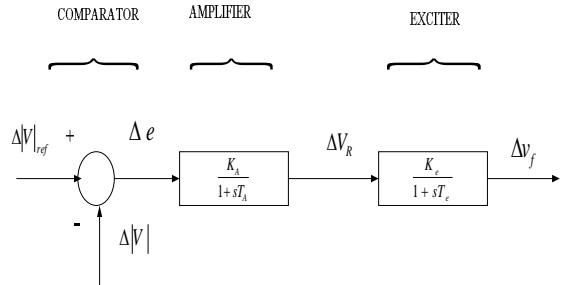


Figure.5: Linear model of the comparator-amplifier-exciter portion of the AVR Loop [4]

After Laplace transformation the last equation yields the field transfer function

$$\frac{\Delta E(s)}{\Delta v_f(s)} = \frac{\Delta|V|(s)}{\Delta v_f(s)} = \frac{K_F}{1+sT_{d0}} \tag{24}$$

where

$$K_F = \frac{\omega L_{fd}}{\sqrt{2}R_f} \tag{25}$$

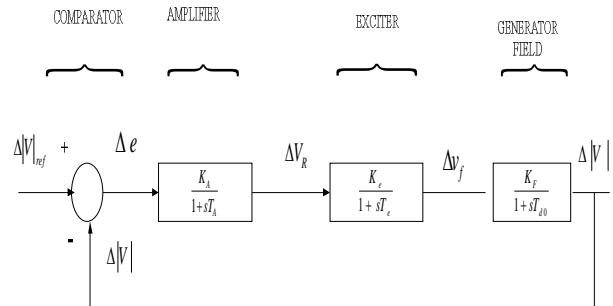


Figure.6: Closing of the AVR loop [4]

and $T'_{d0} = \frac{L_{ff}}{R_f}$

After completing the AVR loop in the above fig. The open loop transfer function G(s) is given by

$$G(s) = \frac{K}{(1+sT_A)(1+sT_e)(1+sT'_{d0})} \tag{26}$$

Where, the open loop gain K is defined by

$$K \cong K_A K_e K_f \tag{27}$$

4.4 Development of AVR with Damper Circuit

In case of positive damping that mainly originates in the rotor damper windings the oscillations in all probability would be

signal to use for controlling generator excitation is the speed deviation.

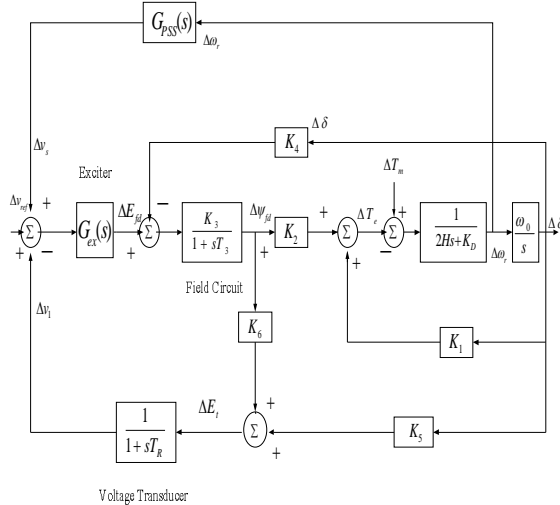


Figure.9: Block Diagram of AVR and PSS [7]

The theoretical basis of a PSS may be illustrated with the above block diagram in figure 9. The system contains a generating unit connected to an infinite bus through a transformer and a pair of transmission lines. The terminal voltage of the generator is connected with the help of an excitation system and AVR. An associated governor monitors the shaft frequency and thus controls the mechanical power.

6 FUZZY CONTROL BASED CO-ORDINATED AVR-PSS SYSTEM:

FUZZY SETS

It is a set without a crisp boundary. The transition from ‘belong to the set’ to ‘not belong to the set’ is gradual and smooth. The fuzzy set theory is based on fuzzy logic where a particular object has a degree of membership that is in the range of 0-1.

6.1 Fuzzy Logic

Fuzzy logic is a powerful tool in many engineering applications that require less computation and no exact mathematical model of the system. It is conceptually easy to understand and flexible and represent in figure 10 and 11. Fuzzy logic has four main parts: fuzzification interface, knowledge base, decision making logic and defuzzification interface.

- **Fuzzification interface:** it is the process of mapping inputs to fuzzy sets in the various input universe of discourse the mapped data are converted to linguistic terms. The Fuzzy Logic Controller block implements a fuzzy inference system (FIS) in simlink.
- **Knowledge base:** it consists of a data base and linguistic control rules. The data base provides necessary definitions, which are used to define the linguistic control rules and fuzzy data manipulation in a FLC.
- **Decision making:** it has the ability of simulating human decision making based on fuzzy concept.

- **Defuzzification:** it converts the output values into non fuzzy logic decision system.

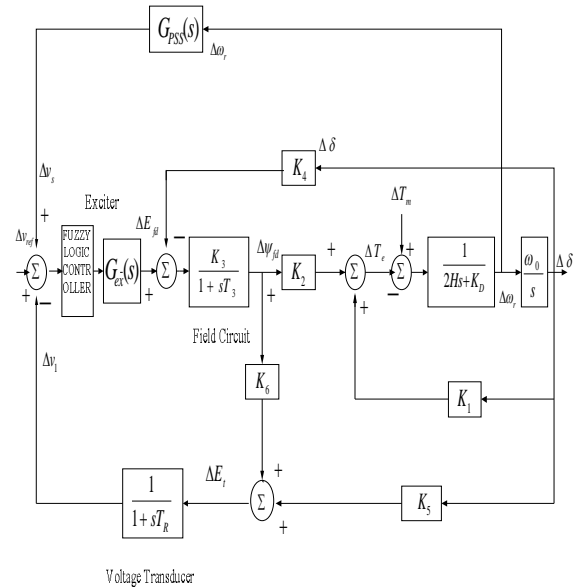


Figure.10: Block diagram of AVR with PSS in fuzzy logic [8]

The detail of the fuzzy logic based AVR-PSS system is shown in the above model.

6.2 Fuzzified Ideal AVR Model

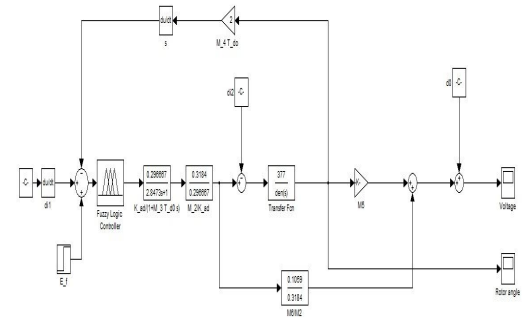


Figure 11: Simulink Block Diagram of Fuzzified Ideal AVR Model

CHANGE IN VOLTAGE:

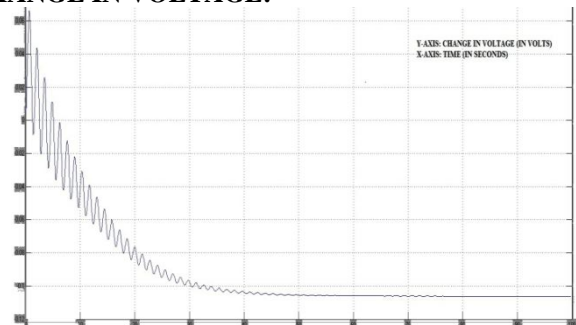


Figure.12: Output (Change in Voltage) of the Fuzzified Ideal AVR Model

CHANGE IN ROTOR ANGLE

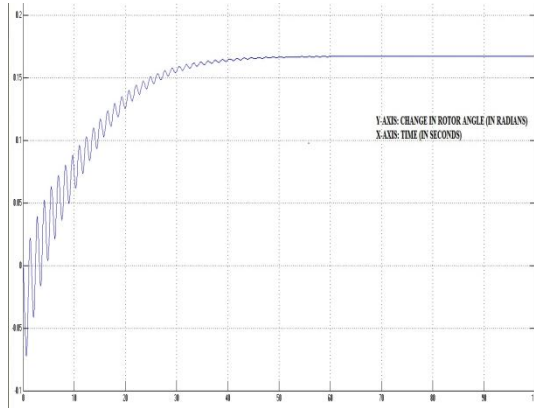


Figure.13: Output (Change in Rotor Angle) of the Fuzzified Idea AVR Model

The above results of figure 11 represent simulink Block Diagram of Fuzzified Ideal AVR Model. Figure 12 depicts output change in Voltage of the Fuzzified Ideal AVR Model and figure13 represents output change in rotor angle of the Fuzzified Idea AVR Model.

TABLE 1 IEEE MACHINE DATA

[Specifications for single area system model of conventional Heffron-Phillips and the Ideal AVR model]

Sl.No.	PARAMETERS	VALUES
1.	R_e	0
2.	X_e	0.5
3.	V_t	1
4.	V_∞	1.05
5.	H	3.2
6.	T_{d0}	9.6
7.	K_A	400
8.	T_A	0.2
9.	X_q	2.1
10.	X_d	2.5
11.	X_d'	0.39
12.	D	0.05
13.	Ω	377
14.	Δ	65.52
15.	I_d	0.4014
16.	I_q	0.3675
17.	V_d	0.7718
18.	V_q	0.6358
19.	E_q	0.7923
20.	E_{fd}	1.6392
21.	T_M	0.5434
22.	K_1	0.9224

23.	K_2	1.0739
24.	K_3	0.2966
25.	K_4	2.2655
26.	K_5	0.005
27.	K_6	0.3572
28.	M_1	0.1282
29.	M_2	0.3184
30.	M_3	0.2966
31.	M_4	-0.6721
32.	M_5	-0.7413
33.	M_6	0.1059
34.	M_7	0.5811
35.	M_8	0.07111
36.	M_9	-0.1432
37.	M_{10}	0.3472
38.	M_{11}	-0.0375
39.	M_{12}	-0.2909
40.	D_{i1}	-0.0464s
41.	D_{i2}	0.0154
42.	D_0'	0.0058

7. RESULTS AND DISCUSSIONS

Table 2: Comparison of Rotor Angle Response

SL. NO.	IDEAL AVR MODEL	PROPOSED FUZZIFIED AVR MODEL
1.	0.1282	0.1674
2.	1.39 s	1.39 s
3.	20.69 s	30.39 s
4.	27.59 s	37.4 s
5.	0.0001	0.0001

Here a block diagram model is considered for the stability analysis of rotor angle and voltage. The IEEE data for machine parameter is given in the Table 2 the rotor angle response of the machine has been studied by simulating the Ideal AVR model and the fuzzified ideal AVR model.

8. CONCLUSION

The ideal AVR model exhibits the best maximum overshoot, while the fuzzified ideal AVR has a better overshoot. The peak is achieved at the same time in the ideal AVR model as well as the proposed fuzzified model. The settling time period in both the 5% and 2% criteria is least in the ideal AVR model; the proposed fuzzified model has a comparable settling time period which is faster. Finally the steady state error has been observed to be the same in the ideal AVR and its proposed fuzzified model, which is again better model.

REFERENCES

1. Heffron, W. G. Philips, R. A., **Effect of a modern voltage regulator on under-excited operation of large turbine generators.** AIEE Transaction 71:692-97.1952.
<https://doi.org/10.1109/AIEEPAS.1952.4498530>
2. P. Kundur, **Power System Stability and Control**, Mc-Graw Hill-1994.
3. Olaf Samuelsson, **“Power system damping,” structural aspects of controlling active power.**
4. M. G. McArdle, D. J. Morrow, P. A. J. Calvert, O. Cadel, **“Modern semiconductor technology,”**
5. DeMello. F. P. Concordia. C., **Concepts of synchronous machine stability as affected by excitation control,** IEEE Transaction PAS-88:316-29, 1969.
<https://doi.org/10.1109/TPAS.1969.292452>
6. Anderson, P. M., Fouad, A. A., **Power System Control & Stability**, Iowa State University Press, Iowa, 1977.
7. P. Kundur, M. Klein, G. J. Rogers and M. S. Zwyno, **“Application of Power System Stabilizer for enhancement of Overall System Stability,”** IEEE Trans., Vol PWRS-4, pp. 614-626, May 1989.
<https://doi.org/10.1109/59.193836>
8. P. Kundur, J. Paserba, V. Ajarapu, G. Anderson, A. Bose, C. Canizares, N. Hatziaargyriou, D. Hill, A. Stankovic, C. Taylor, T. VanCutsem, and V. Vital, **“Definition and classification of power system stability,”** IEEE Trans. Power Syst., Vol. 19, no. 2, pp. 1387-1401, May 2004.
<https://doi.org/10.1109/TPWRS.2004.825981>
9. Olle I. Elgerd, **“Electric Energy Systems Theory An Introduction”**, 2nd edition, Tata Mc-Graw Hill Publication, New-Delhi, 1983.
10. Maria Zemzami, Norelislam Elhami, Mhamed Itmi, Nabil Hmina, **“An evolutionary hybrid algorithm for complex optimization problems”**, International Journal of Advanced Trends in Computer Science and Engineering, 8(2), March -April 2019, 126-133.
<https://doi.org/10.30534/ijatcse/2019/05822019>
11. Maria Zemzami, Norelislam Elhami, Mhamed Itmi, Nabil Hmina, **“Interoperability Optimization using a modified PSO algorithm”**, International Journal of Advanced Trends in Computer Science and Engineering, 8(2), March -April 2019, 101-107.
<https://doi.org/10.30534/ijatcse/2019/01822019>
12. Ganthia, B.P.; Rana, P.K.; Pattanai, S.A. **“Space Vector Pulse Width Modulation Fed Direct Torque Control of Induction Motor Drive Using Matlab-Simulink”**. In Proceedings of the 3rd International Conference on Electrical, Electronics, Engineering Trends, Communication, Optimization and Sciences (EEECOS), Tadepalligudem, India, 1–2 June 2016.
13. Ganthia B.P., Pritam A., Rout K., Singhsamant S., Nayak J. (2018) **Study of AGC in Two-Area Hydro-thermal Power System.** In: Garg A., Bhoi A., Sanjeevikumar P., Kamani K. (eds) *Advances in Power Systems and Energy Management. Lecture Notes in Electrical Engineering*, vol 436. Springer, Singapore.
https://doi.org/10.1007/978-981-10-4394-9_39
14. B. P. Ganthia, R. Pradhan, S. Das and S. Ganthia, **“Analytical study of MPPT based PV system using fuzzy logic controller,”** 2017 International Conference on Energy, Communication, Data Analytics and Soft Computing (ICECDS), Chennai, India, 2017, pp. 3266-3269.
15. Bibhu Prasad Ganthia, Prashanta Kumar Rana, Tapas Patra, Rosalin Pradhan, Rajashree Sahu, **Design and Analysis of Gravitational Search Algorithm Based TCSC Controller in Power System**, Materials Today: Proceedings, Volume 5, Issue 1, Part 1, 2018, Pages 841-847, ISSN 2214-7853,
<https://doi.org/10.1016/j.matpr.2017.11.155>.
16. Bibhu Prasad Ganthia, Aditi Abhisikta, Deepanwita Pradhan, Anwes Pradhan, **A Variable Structured TCSC Controller for Power System Stability Enhancement**, Materials Today: Proceedings, Volume 5, Issue 1, Part 1, 2018, Pages 665-672, ISSN 2214-7853,
<https://doi.org/10.1016/j.matpr.2017.11.131>.
17. B. P. Ganthia, S. Mohanty, P. K. Rana, P. K. Sahu, **“Compensation of voltage sag using dvr with pi controller”**, Electrical Electronics and Optimization Techniques (ICEEOT) International Conference, pp. 2138-2142, 2016.
<https://doi.org/10.1109/ICEEOT.2016.7755068>
18. Ganthia Bibhu Prasad and Rout Krishna 2016 **DEREGULATED POWER SYSTEM BASED STUDY OF AGC USING PID AND FUZZY LOGIC CONTROLLER** *Int. J. of Adv. Res.* 4 847-855 www.journalijar.co
<https://doi.org/10.21474/IJAR01/823>